Experimental Study on Diesel Particulate Filter with Reciprocating Flow

Yangbo Deng*, [1], Xiaolong Wang[2], Guangquan Chen[2], Hongwei Wu[3], Zhitao Han[2], Rongrui Li[2]

[1] Naval Architecture and Ocean Engineering College, Dalian Maritime University, Dalian116026, China

[2]Marine Engineering College, Dalian Maritime University, Dalian116026, China

[3]School of Engineering and Computer Science, University of Hertfordshire, Hatfield, AL10 9AB, UK

ABSTRACT: In this article, a new diesel particulate filter (DPF) system with reciprocating flow is proposed and an experimental study on the characteristics of the active-passive component regeneration of the DPF system was carried out. The temperature, pressure difference and pollution emissions of the DPF system are measured under stable operation conditions. The process of treating pollution and regeneration of the DPF system as well as the effects of reciprocating flow cycle on the performance of the DPF system are analyzed. Results show (1) the DPF system can use the pollutants in emissions and a tiny amount of extra fuel to maintain the chemical reaction, periodically releasing heat and storing heat and reversely blowing away ash, which in turn realize the regeneration of the cDPF. (2) with the reciprocating flow cycle increasing, the temperature profile moves parallel toward the downstream side of the DPF system and the fluctuating range of CO、NO and NO_2 components increases. (3) if a reasonable temperature in upstream DOC and cDPF during each half cycle is formed, the regeneration efficiency of the DPF system can be obviously improved and the average content of PM emission can be kept at a quite low level.

Keywords: Experimental study; Diesel particulate filter; Regeneration; Particulate matter; Reciprocating flow

■ INTRODUCTION

Nowadays, the negative influence of particulate matter (PM) emission from diesel engines on human health and environment attracts more and more attention in recent years[1,2]. Thus, many countries have established strict statutes and restrictive standards to limit PM emission of engines. These increasingly stringent regulations are driving manufacturer efforts to develop efficient after-treatment techniques which can remove the PM emission from diesel engine[3,4]. It is recognized that the most widely used approach to remove PM emission from diesel engine is diesel particulate filter (DPF)[5].

Although a typical wall-flow DPF can remove PM in excess of 95% over a wide range of engine[6], the DPF is designed to keep a certain quantity of PM. The overloaded PM would create a blockage to the flow through the DPF, eventually produce excessively high pressure drop of the flow through the DPF and prevent the engine operation properly[7]. Therefore, the DPF needs to be designed to provide a reliable way of removing accumulated PM from the filter to restore its PM collection capacity[8]. Removing PM is known as the regeneration of DPF, which is a main technical challenge in the practice application of the DPF.

There are mainly two types of regenerations of DPF: active regeneration and passive regeneration. Active regeneration periodically removes the PM trapped in a DPF through a controlled oxidation with O_2 at 550℃or higher temperatures[9]. In this case, the heat must be supplied from outside sources, such as an electric heater, a microwave heater and a flame-based burner[10]. The external energy that used for heating would increase the cost of a DPF system due to complex supplements[11]. On the other hand, the passive regeneration utilizes ongoing catalytic reaction at the exhaust gas temperature to oxidize the PM trapped in a DPF without additional fuel. Diesel Oxidant Catalyst (DOC) assisting DPF regeneration is a typical of passive regeneration method which is also named as continuously regenerating trap (CRT) system. The CRT system is installed with a DOC where NO is preferentially converted to NO_2 before a DPF and NO_2 is used to oxidize PM trapped in the filter below 300 °C[12]. In order to achieve the best performance, however, the CRT system should satisfy two conditions which the temperature is in the range 250–450 °C and NOx/Soot ratio is adequately high. Otherwise the produced NO_2 will be too low to oxidize soot. It should be noticed that both HC and CO would be the secondary pollution from incomplete oxidation conversion of the soot in the CRT system.

It needs to be mentioned that both active regeneration and passive regeneration of the DPF cannot keep the filter clean in a long term. In order to overcome this problem, the active-passive component regeneration of DOC assisting DPF is a traditional option[13]. A certain amount of fuel is injected into the cylinder in the late stage of combustion process, or a certain amount of fuel is injected into the exhaust pipe at the upstream of a DOC[14-16]. The DOC is used to oxidize the fuel, heat the downstream DPF and realize the passive regeneration of DPF. In-cylinder injection of the fuel has an advantage that no additional fuel injection device is needed, whereas a main disadvantage is that the lubricating oil of the diesel engine will be diluted by the fuel. In-exhaust-pipe direct injection can avoid oil dilution, which becomes the main technical approach of the active-passive component regeneration of DOC assisting DPF.

It is known that the active-passive component regeneration of DOC assisting DPF should maintain the temperature in the DOC and DPF within a suitable range. The temperature in DOC should be kept in the range of 250–450 ℃ then NO is preferentially converted to NO_2. While the temperature in DPF should be high enough to effectively burn the accumulated soot in the DPF and kept below a certain threshold to prevent the DPF from being damaged. As a result, this regeneration method will be facing a challenge on how to control the temperature in the DOC and DPF. This is due to the fact that several factors need to be concerned, they are the wide range of engine operations, thermal inertia of DOC and DPF, the complexities of the reactions in DOC and DPF, and the injection model of the fuel injectors[17,18].In addition, all forms of DPF regeneration can only remove combustible constituents without removing incombustible constituents remaining behind as ash in the PM trapped. After a long period of operation, the DPF still needs to be disassembled to clean up the residues in filter[19-21].

A reciprocating flow regeneration (RFR) has also been identified to be an effective means to realize active-passive component regeneration of the DPF utilizing a tiny amount of additional fuel[22,23]. RFR exploits heat recovery properties to provide a high temperature region that maintains the regeneration of the filter. However, the temperature gradients at the inlet and outlet of the DPF not only defer regeneration process deferment but also result additional thermal stress. To address these issues, Zheng et al. proposed an RFR structure that two inert monolith blocks with flow-through passage are installed at the both ends of a DPF[24]. The monolith blocks can enhance the heat recuperation, reduce the temperature gradient and maintain a more

stable temperature profile in the DPF. Furthermore, Zheng et al. improved the RFR configuration with two DOCs plus non-catalytic DPF[25]. The DOCs are placed at location favorable for catalytic activity with RFR operation to maintain the catalytic light-off temperature. The improved RFR device under operation conditions has significant advantage in supplemental energy saving as compared to standard DOC and DPF configuration.

RFR is a highly complex chemical reaction process that combines periodically reciprocating flow, particulate matter separation, multiphase reactions, heat and mass transfer over a range of temporal and spatial domains. To the best knowledge of the authors, there are few open published reports in applying the concept of periodically reciprocating flow to the exhaust after treatment system of diesel engine. There is also no literature on investigating the mechanism of the new DPF system combining the RFR with the component regeneration of DOC assisting DPF. There is still much room to be investigated further in this research area.

In the current work, a new DPF system based on the concept of combining the RFR with the active-passive component regeneration of DOC assisting DPF is proposed and designed. The proposed new DPF system consists of a catalyzed diesel particulate filter (cDPF) and two DOCs. There is a space interval between every DOC and the cDPF. The new DPF system uses periodically reciprocating flow, chemical reaction, releasing heat and storing heat to form a stable temperature distribution that a high temperature region is located in central DPFs and two low temperature regions are located in the DOCs on both sides. The new DPF system use a small amount of extra fuel to maintain the oxidation conversion of the soot trapped, use a downstream DOC to oxide HC and CO from incomplete oxidation conversion of soot, and utilize the reverse flow to blow away the ash accumulated. Furthermore, we will experimentally study the temperature distribution, the treatment of pollution, the fundamental principles to realize the reciprocating flow regeneration in the new DPF system and the effects of reciprocating flow cycle on the performance of the DPF system.

■ EXPERIMENTAL APPARATUS AND METHOD

Experimental Apparatus. As shown in Figure 3, the experimental system mainly consists of a diesel engine, exhaust lines, a DPF system, and measurement system.

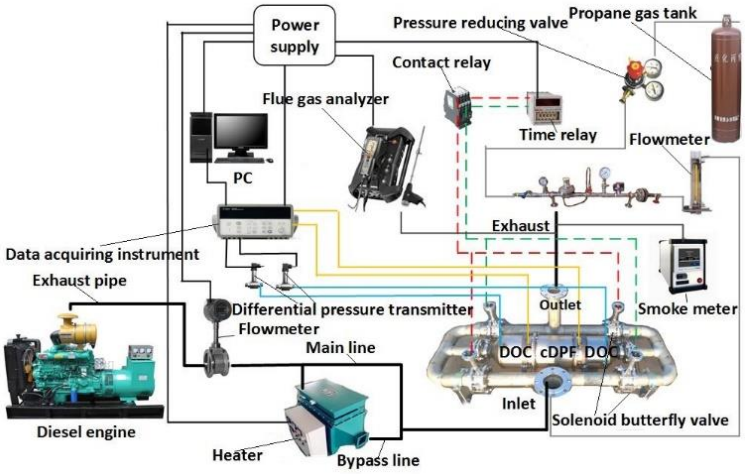

Figure 1. Schematic diagram of experimental set up

The diesel engine is a six cylinder in-line with water cooling, turbo-charging and inter-cooling, four strokes direct injection heavy-duty diesel engine. The main specifications of the engine are given in Table 1. The diesel engine burns 0# diesel oil (National V emission standard) and is operated under idle condition.

The DPF system is composed of two diesel oxidation catalysts (DOCs), a catalyzed diesel particulate filter（cDPF）and flow lines in Figure 2. Two DOCs are symmetrically arranged on both sides of the cDPF and a structure of DOC+cDPF+DOC is formed. Two pairs of solenoid butterfly valves synchronously opening and closing in the flow lines control the periodically reciprocating flow of the airflow in the DPF system.

Table 1. Diesel engine characteristics

Compression ratio	16:1
Cylinder diameter × stroke	105×130mm
Number of cylinders	6
Total piston displacement	6.75L
Rated speed	1500r/min
Calibration power	110kW
Full load exhaust temperature	≤540□～600□

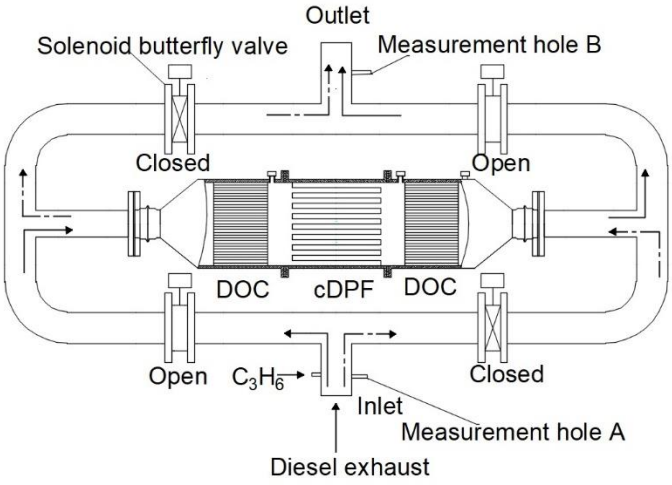

Figure 2. Schematic diagram of DPF system

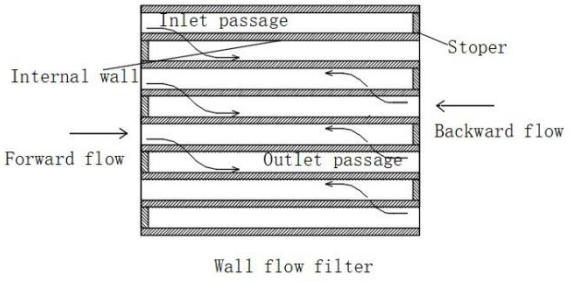

Figure 3. Schematic diagram of wall flow filter

Table 2. Characteristics of DOC and cDPF

	DOC	cDPF
Pore density / cpsi	300	200
Main material	Cordierite	Cordierite
Porosity/%	35-40	50-60
Wall thickness of channel / mm	0.25	0.3
Average pore diameter / mm	3-7	8-20
Noble metal catalysts	Pt,Pd	Pt,Pd
Catalyst load / ($g.m^{-3}$)	706.2	353
Catalyst carriers	Al_2O_3 + $Ce(Zr)O_2$	Al_2O_3 + $Ce(Zr)O_2$
Length/mm	152.4	254
Diameter/mm	240	240

Each DOC is a cordierite ceramic monolith that has a honeycomb structure with parallel channels. Al_2O_3 and $Ce(Zr)O_2$ catalyst carriers coat the channel walls and support metal Pt/Pb catalysts. As shown in Figure 3, the filter of the cDPF is a wall flow filter with the alternate channels plugged at one end and open at the

opposite end. The cordierite particles sintered together form the porous matrix of the internal wall between the alternate channels. The wall flow filter is also coated a layer of Al_2O_3 and $Ce(Zr)O_2$ as catalyst carriers and the catalyst carriers support metal Pt/Pb catalysts. The characteristics of the DOC and the cDPF respectively are given in Table 2. Both DOC and cDPF use bimetallic Pt-Pb catalysts that the ratio between Pt and Pb is 4:1. The Pt in the catalysts can enhance NO oxidation to NO_2. Small amount of Pb can improve the thermal stability of the catalysts and reduce the light-off temperature of soot, CO and HCs oxidation.

The exhaust lines extend from the engine exhaust pipe to the DPF system and include a main line and a bypass line with a 30 KW electrical heater. Because the exhaust temperature of 396 K at the inlet is insufficient to initiate a thermal regeneration, supplemental energy will be applied to raise the exhaust gas or the DPF substrate temperature. When the exhaust gas flows into the DPF system through the bypass line, electrical heater is used to heat the exhaust gas. When the exhaust gas flows into the DPF system through the main line, a tiny amount of propane gas as additional fuel is introduced at the inlet of the DPF system in the experiments. The propane gas is chosen as additional fuel in the experiment in order to facilitate using flue gas analyzer to measure the components in the exhaust gas. In order to ensure the measurement accuracy, 99.9% pure propane gas used.

The flow of the exhaust gas is measured using vortex flowmeter and the flow of propane gas is measured using a glass rotameter. The pressure upstream and downstream of the DPF system, the pressure upstream of the exhaust line, and the ambient pressure are measured using piezoresistive pressure transmitters. The temperature at different locations of the DPF system, the upstream temperature of the exhaust line and the ambient temperature are measured using K-type thermocouples. The thermocouples are also arranged along the axis of the DOCs and cDPF, wich can be used to measure the temperature of the channel walls along the axis in the DOCs and cDPF.

The emissions and particulate concentrations in the exhaust line are measured respectively using a Testo350 flue gas analyzer and a SMG smoke meter at the inlet and outlet of the DPF system. The measure point of the inlet is set at measurement hole A and the measure point of the outlet is set at measurement hole B in Figure 2. An Agilent 34970A data acquisition instrument is used to acquire the experimental data and transmit the data into a PC.

Experimental Method. At the startup of the DPF system, the main line is closed while the bypass line is opened. The electrical heater is used to heat the exhaust gas to the required temperature starting the DPF system and a certain amount of propane gas is introduced at the inlet. As the reasonable temperature distribution in the DPF system is established, the main line is opened and the bypass line is closed. The temperature changes at the several measuring points in the DPF system with periodically reciprocating flow are observed. When the temperatures periodically fluctuate and the fluctuating amplitude are nearly equal at every measuring point, the DPF system is considered to be in stable operation conditions, and the experimental parameters including temperature, pressure, pollution emissions concentrations and particulate concentrations are measured accordingly.

During the experiment, the reciprocating flow cycle in the DPF system is separately 30s, 50s, 70s and 90s, the volume flow of exhaust gas is kept at 248.3 m^3/h, the volume flow of the propane gas introduced at the inlet is 0.18 m^3/h, the exhaust temperature is 396 K at the inlet, and the components of exhaust gas at the inlet of the DPF system are listed in table 3.

Table 3. Components of exhaust gas at inlet

O_2/%	CO/ppm	NO/ppm	NO_2/ppm	NO_x/ppm	SO_2/ppm	PM/mg/m^3	HC/ppm
17.9	394	208	41.2	249.2	88	256	195

The mean concentration of particulate matter, CO emission, HC emission and the mean pressure difference at the outlet of the DPF system are the average value of the parameters measured in 30 reciprocating flow cycles as the DPF system maintain stable operation at the reciprocating flow cycle set.

Uncertainty Analysis of Experimental Results. The uncertainties of the measurements in the experiment are dependent on the experimental conditions and the measurement instruments. The accuracy and alongside other details of the measuring instruments used in the experiment are listed in Table 4. An uncertainty analysis is performed on the experimental results using the propagation of error method described by Moffat[26]. The uncertainty of the temperature measurement is ±1.5 K, the uncertainty of the pressure measurement is ±2.0 Pa, the uncertainty of the flow measurement of the exhaust gas is ±3.75 m^3/h, the uncertainty of the flow measurement of the propane gas is ±0.005 m^3/h, the measurement uncertainty of the emissions concentrations is ±10 mg/m^3 and the measurement uncertainty of the particulate concentrations is

±10 mg/m^3.

Table 4. Measuring instrument characteristics

Instrument	Performance parameter	Manufacturer and model	Precision
Vortex flowmeter	Range 100 ~ 1000 m^3/h	LUGB-23100C	1.5%
Glass rotameter	Range 0.01 ~ 0.6 m^3/h	Propane gas	2.5%
Pressure transmitter	Range 0 ~ 10KPa, Sensitivity 1.6mA/KPa	Keller PD-23/8666.1/ 0.1	Linearity <0.10%FS
Thermocouple	Variety Ni-Cr-Si/Ni-Si, Φ0.5×500mm×L1500mm	WRNK-162	±1.5 K
Flue gas analyzer	Response time O_2<20s, Response time CO<40s, Response time HC<40s, Response time NO <30s, Response time NO_2<40s,	Testo 350	O_2,0.2Vol.% CO,5% of reading HC,10% of reading NO,5% of reading NO_2,5% of reading
Smoke meter	Range 5 ~ 500mg/m^3, Particle size 0.1μm ~ 10μm, Response time <15s	SMG100	5%
Data acquisition	Scan speed60 channels/s	Agilent 34970A	DC voltage 0.002% Temperature 1□

■ ANALYSIS OF RECIPROCATING FLOW REGENERATION

As the DPF system maintains stable operation utilizing a tiny amount of propane gas as additional fuel, the DPF system can filter the particulate, remove the CO and HC emissions and realize regeneration under the condition of periodically reciprocating flow, as shown in Figure4.

During the forward flow cycle T_f, the diesel exhaust gas is introduced in first DOC from the left sides, flow through cDPF and second DOC in turn. The conversion of carbon monoxide (CO) can reach to 90% and the conversion of hydrocarbon (HC) can reach to 80% at 623 *K* in DOC[27]. Consequently, the propane gas as additional fuel, the CO and HC in the exhaust gas are oxidized into H_2O and CO_2 by the residual oxygen of the exhaust gas in first DOC. The hydrocarbons oxidized also include the volatile constituents adsorbed in the particulate matter. The volatile constituents are mainly soluble organic fraction (SOF) and release from the particulate matter at T_{sof}=346 *K*[6]. At the same time, the nitrogen monoxide (NO) is partially converted into the nitrogen dioxide (NO_2) in the exhaust gas in first DOC.

As the diesel exhaust gas flow through the cDPF, the particulates contained in exhaust gas are trapped and deposited on the walls of inlet passages during the T_f , as shown in Figure 3 and Figure 5. After the DPF system is started, the temperatures in the cDPF can keep higher than 823 K. The temperature of light off of

soot oxidation is T_{l2}=873 *K* in loose contact between the soot and catalyst and is T_{ll}=693 K in intimate contact in cDPF[28-31]. The soot particulates on the walls are oxidized into CO_2 and the residual ash particles are remained on the walls of the inlet passages in the cDPF, as showed in Figure 3 and Figure 5[32,33]. The short residence time results in the incomplete soot oxidation and the rapid CO generation in the cDPF. The CO from cDPF is oxidized into CO_2 in second DOC.

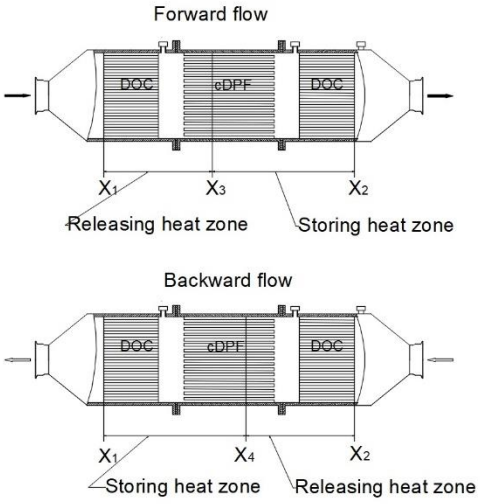

Figure 4. Heat-stored and heat-rejected zone during a cycle

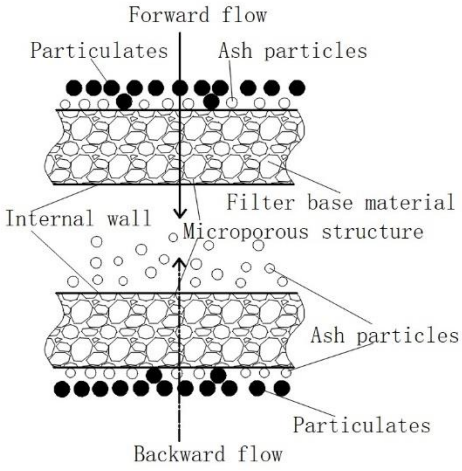

Figure 5. Schematic diagram of filtering particulates

In the upstream region of the DPF system, the solid frame in the first DOC and the cDPF has higher temperature than the diesel exhaust gas. The solid frame in the region releases heat to the exhaust gas during

the T_f, as illustrated in Figure 4. In the downstream region of the DPF system, the chemical reaction in the cDPF and the second DOC releases heat to the solid frame and the heat is stored in solid frame of the storing heat region. The amount of thermal storage in the solid frame during the T_f is described by the Eq 1.

$$Q_s = \int_0^{T_f} q_s \, d\tau \qquad (1)$$

$$q_s = \int_{X_3}^{X_2} \rho_s \, c_s \frac{dT_s}{d\tau} dx \qquad (2)$$

During the backward flow half cycle T_b, the diesel exhaust gas is introduced in the second DOC from the right sides, flow through cDPF and the first DOC in turn. During the T_b, the solid frame in the storing heat region during previous T_f releases heat to the exhaust gas and activate the same chemical reactions in the new upstream region of the DPF system as in previous T_f, see Figure 4. The releasing heat in the new releasing heat region during the T_b is described by the Eq 3.

$$Q_R = \int_0^{T_b} q_R \, d\tau \qquad (3)$$

$$q_R = \int_{X_4}^{X_2} \rho_s \, c_s \frac{dT_s}{d\tau} dx \qquad (4)$$

During the T_b, the particulates contained in exhaust gas are trapped and deposited on the walls of the outlet passage of the cDPF, as demonstrated in Figure 3 and Figure 5. The soot in the particulates accumulated is oxidized and the residual ash particles are remained on the walls of the outlet passages. At the same time, the residual ash particles on the walls of the inlet passages during the previous T_f are stirred, blown away and carried away by reverse flow, as showed in Figure 5.

During the T_b, the chemical reactions release heat to the solid frame in the new downstream region of the DPF system. The amount of thermal storage of the new storing heat region during the T_b is described by the Eq 5.

$$Q_S = \int_0^{T_b} q_S \, d\tau \qquad (5)$$

$$q_S = \int_{X_1}^{X_4} \rho_s \, c_s \frac{dT_s}{d\tau} dx \qquad (6)$$

The same process of the storing heat and releasing heat in the same location is repeated in next reciprocating flow cycle. The DPF system with reciprocating flow can use the pollutants in emissions and a tiny amount of extra fuel to maintain the chemical reaction, periodically releasing heat and storing heat,

reversely blowing away ash. These make the DPF system not only effectively remove the air pollutants such as CO, HC and PM in the exhaust gas, but also realize the continuous active-passive component regeneration of the cDPF.

■ RESULTS AND DISCUSSION

Temperature Profiles during A Reciprocating Flow Cycle. As the reciprocating flow cycle is 50s, the changes of temperature profiles along the axial direction in DPF system during a reciprocating flow cycle are displayed in Figure 6. A trapezoidal temperature profiles is formed, and the high temperature region lies in the middle (-277.5 $mm \leq X \leq 63.5$ mm) and the high temperature gradients locate on both sides along axial direction during each half cycle. The temperatures in the cDPF always keep higher than the temperature of lighting off of soot oxidation. Each DOC has a temperature gradient in a range from 360K to 1080K. The high temperature region travels at close to constant speed from the upstream sides of the DPF system towards the downstream side during each half cycle.

At the beginning of the T_f, a temperature maximum can be observed at X=-277.5 mm near the upstream sides of the high temperature region in Figure 6 (a). During the T_f, the temperature in the high temperature region increases, the temperature near the downstream side rises more rapidly and gradually grows into a new temperature maximum at X=0 mm. At the beginning of the T_b after the flow direction switches, the maximum temperature at the end of the previous T_f still occurs near the new upstream side in Figure 6 (b). During the T_b, the temperature within the high temperature region decreases and the temperature near the new downstream side decreases at a slower rate. A new temperature maximum at X=-277.5 mm appears gradually. The downstream maximum will become a new upstream maximum after the next change in the flow direction. The changes of temperature profiles during the T_f are not exactly same with that during the T_b. The main reason could be that an asymmetric temperature distribution along the axial direction of the DPF system is formed in the start-up process of the DPF system.

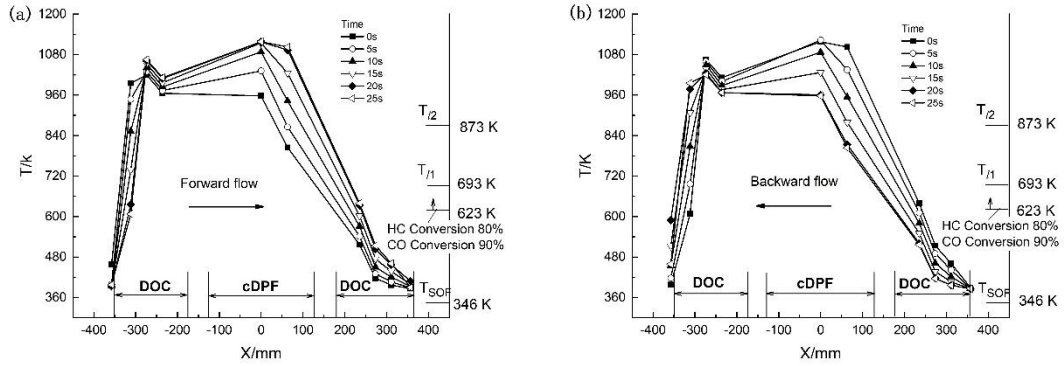

Figure 6. Change of temperature profiles during a forward half cycle, (a) Forward half cycle, (b) Backward half cycle.

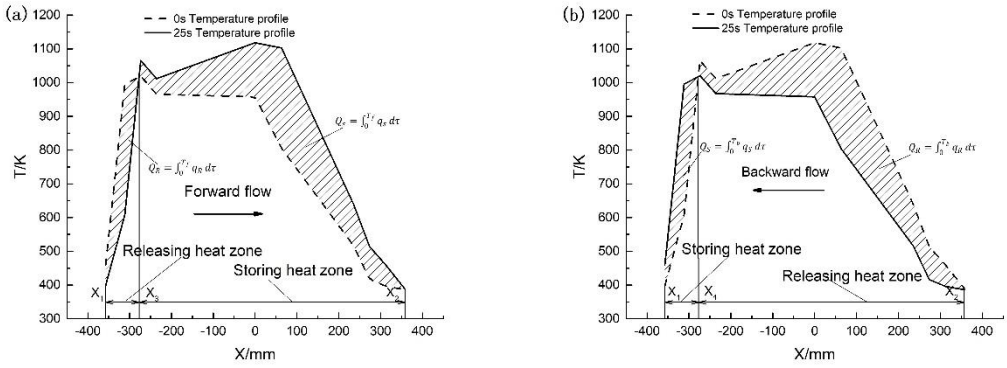

Figure 7. Heat-stored and heat-rejected during a cycle, (a) Forward half cycle, (b) Backward half cycle.

Figure 7 shows the process storing heat and releasing heat during the reciprocating flow cycle. The temperature within the region of -351.5 *mm* ≤*X*≤ -273.5 *mm* decreasing continuously illustrates that the solid frame of the first DOC releases heat to the exhaust gas as a releasing heat region during the T_f in Figure 6 (a). The temperature within the region of -273.5 *mm* ≤*X*≤ 357.5 *mm* increasing continuously illustrates that the chemical reaction releases enough heat to increase the temperature of the exhaust gas and heat the solid frame in the region of the cDPF and second DOC. The amount of thermal storage in the solid frame of -273.5 *mm* ≤*X*≤ 357.5 *mm* during T_f is indicated by the shadow area in Figure 7 (a). The value of the thermal storage is described by the Eq 1.

During the T_b, the temperature within the region of -273.5 *mm* ≤*X*≤ 351.5 *mm* decreases and the heat stored in the region during previous T_f is released to heat the exhaust gas and activate the chemical reactions in

the region in Figure 6 (b). The releasing heat during the T_b is indicated by the shadow area in the region in Figure 7 (b), and its value is described by the Eq 3. The temperature within the region of -351.5 *mm* ≤X≤ -273.5 *mm* increases and the heat released from the chemical reactions is stored in the solid frame of the first DOC in the region. The heat stored during the T_b is indicated by the shadow area in the region in Figure 7 (b) and its value is described by the Eq 5.

Dividing point between endothermic and exothermic regions in the DPF system during the T_f and T_b is located in the same position, that is $X_3 = X_4$. The heat stored in endothermic regions in T_f is equal to the heat released in exothermic regions in T_b within the same regions in Figure 7 (a) and (b). The same process of the storing heat and releasing heat in the same location is repeated in next reciprocating flow cycle.

Chemical Reactions During A Reciprocating Flow Cycle. Figure 8 shows the temperature fluctuation curves at different measuring points in the DPF system. Figure 9 shows the variation profiles of O_2、CO、NO and NO_2 components at the outlet of the DPF system. The CO、NO 、NO_2 and O_2 components at the outlet periodically change with the reciprocating flow in the DPF system. At beginning of each half cycle after the flow direction immediately switched, the lower temperature results in the lower CO conversion in new downstream DOC and the CO components increases rapidly, then and stably decreases with the temperature growth of the new downstream during the half cycle.

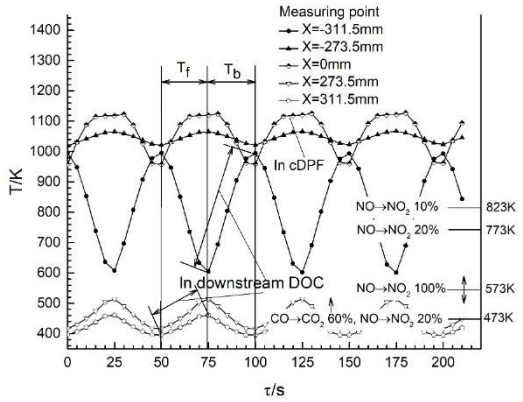

Figure 8. Temperature fluctuation at different measuring points

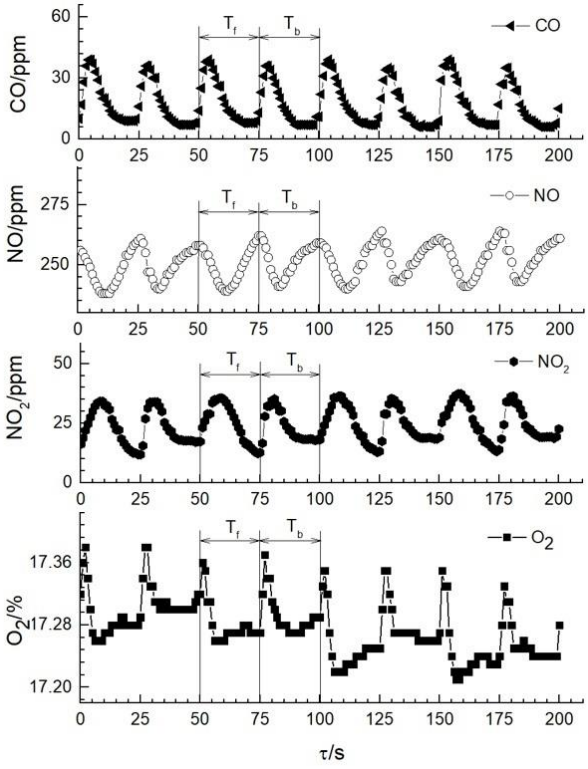

Figure 9. Profiles of O_2、CO、NO and NO_2 at outlet

The variation of NO is associated with NO_2, as is shown in Figure 9. At the beginning of a T_f, the downstream DOC is at lower temperature (400-430*K*) , as is illustrated in Figure 8. The chemical reaction equilibrium of NO_2 and NO is on the NO side in the beginning and then gradually shifts toward the NO_2 side with increasing temperature during the T_f in Figure 9. So, the NO content decreases and the NO_2 content increases with increasing temperature in the range of 433-573 K. After the corresponding conversion is 100% at 573 K, the ratio of NO to NO_2 reduces as the temperature further rises. So, the NO content increases and the NO_2 content decreases with increasing temperature as the temperature is higher than 573 K.

As switching to backward flow, the temperature suddenly approaches to 573 K and the conversion of NO to NO_2 nearly reaches to 100% in new downstream DOC at the beginning of T_b. In this case, the NO content rapidly decreases and the NO_2 content rapidly increases at the beginning of the T_b. Then the NO content increases and the NO_2 content decreases with increasing temperature as the temperature is higher than 573 K in the new downstream DOC. The variation of O_2 is associated with the periodical variations of CO、NO_2、NO and NO_2 component contents in Figure 9.

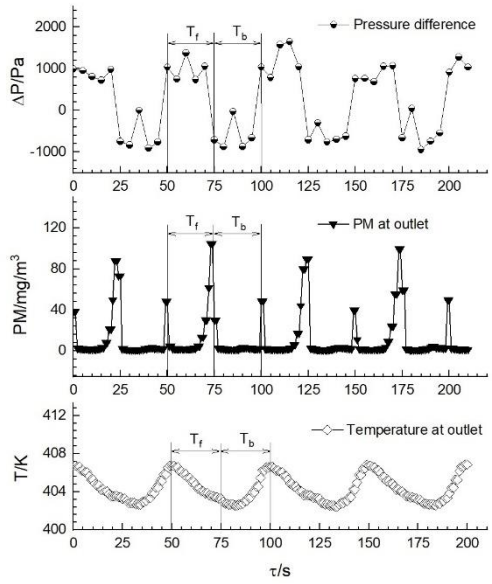

Figure 10. Profiles of ΔP、PM and temperature at outlet

Figure 10 shows the variation profiles of pressure difference ΔP between the inlet and the outlet of the DPF system, particulate matter and temperature at the outlet of the DPF system.

At the beginning of a T_f, the flow passes the inlet passages, the internal wall and the outlet passages in turn in the cDPF. The velocity decreases along the inlet passages gradually. A parts of soot particles in the flow are heated and oxidized into ashes. The ashes can be directly deposited onto the internal walls and form a very thin ash layer used as the substrate for soot particles deposition. Another parts of soot particles in the flow can be deposited onto the thin ash layer and adhered to the internal walls. Because the temperature in the region of X≧-277.53 mm is higher than 623 *K* in first DOC used as upstream DOC, the chemical reaction equilibrium of NO_2 and NO is on the NO side during the T_f. And the temperatures in the cDPF always keep higher than 823 K in Figure 6. Most of soot particles underlain by the thin ash layer are oxidized into ashes further with O_2 alone and without the NO_2 catalytic action. Because of the inertia force, the ash layer and the captured soot particles appears first in the rear part of the inlet channel and then gradually moves to the middle part of the inlet channel during T_f. At the end of the T_f, most of ashes and soot particles incompletely oxidized are accumulated on the internal wall in the rear part of the inlet channel.

As switching to backward flow, the flow passes the outlet passages, the internal wall and the inlet

passages channel in turn. At the beginning of the T_b, the particles carried by the flow in the flow lines, the DOCs channels and the inlet passages of cDPF reversely flow out at the outlet of the DPF system. In addition, the part of residual particles on the internal walls of the inlet passages during the previous T_f are stirred, blown away and carried away by reverse flow as showed in Figure 5. So, the PM content rapidly increases and rapidly decreases in Figure 10.

At the beginning of the T_b, the temperature is lower than 623 *K* in second DOC used as new upstream DOC, the chemical reaction equilibrium of NO_2 and NO is on the NO_2 side. The temperatures near the right end of the cDPF also keep lower than 823 K in Figure 6. According to the published data in references 34, the residual partial particles attached on the walls at rear part of the inlet passages during the previous T_f are stirred, and completely are oxidized into ashes further with the NO_2 catalytic action, rather than are blown away the wall immediately. Then the ashes produced are shifted along the flow path gradually and are carried out by the reverse flow at the end of the T_b. But the content of the ashes produced during every half cycle is too little to influence the PM emission content of the DPF system. At same time the flow state, deposition and distribution of PM in the outlet passages during the T_b, is same to that in the inlet passages during previous T_f. As switching to next forward flow, the PM content rapidly increases, then and rapidly decreases in Figure 10.

In next T_f, because of the temperature distribution in the first DOC and the cDPF, the residual partial soot particles attached on the walls at rear part of the outlet passages the during the previous T_b are only incompletely oxidized into ashes further with O_2 alone. Then the residual partial soot particles attached on the walls of the outlet passages are shifted along the flow path gradually and are carried out by reverse flow at the end of the T_f. So, the PM content rapidly increases late in the T_f. As switching to next backward flow, the PM content rapidly increases to a peak value, then and rapidly decreases in Figure 10.

The pressure difference between the inlet and outlet periodically fluctuate and the fluctuating amplitude of the pressure difference is nearly equal in Figure 10. This illustrates that the particulate accumulation balances with soot oxidation and reverse cleaning in cDPF.

Thus, it can be seen, if the reasonable temperature in upstream DOC and cDPF in one reciprocating flow half cycle is formed, the regeneration efficiency can be improved in the reciprocating flow regeneration

process of the DPF system.

Influence of Reciprocating Flow Cycle. Figure 11 shows the influence of reciprocating flow cycle on the temperature profiles along the axial direction in DPF system. The experiment conditions during every reciprocating cycle are same with above experiment conditions including the flow, components and temperature of the exhaust gas, and the flow of the propane gas. The temperature profiles are shown at the end of every forward half cycle in Figure 11. With the reciprocating cycle increasing, the whole temperature profile moves almost parallel toward the downstream side and high temperature region slightly becomes wider.

Figure 12 shows the corresponding profiles of CO、NO and NO_2 components at the outlet for different reciprocating cycles. Table 5 shows average components of exhaust gas at the outlet of the DPF system for different reciprocating cycles.

The periodical change regulation of CO、NO and NO_2 components at the outlet with the reciprocating flow are consistent with each other. For every reciprocating cycle, at beginning of each half cycle after the flow direction immediately switched, the lower temperature in new downstream DOC results in the lower CO conversion and the CO components increases rapidly, then and stably decreases with the temperature growth of the new downstream DOC during the half cycle. Because the whole temperature profile moves toward the downstream side with the reciprocating cycle increasing, the temperature maximum of the downstream DOC increases and the temperature difference between the downstream DOC and upstream DOC increases during a half cycle. So the peak value of the CO emission fluctuation increases, the efficiency of CO conversion increases and the average CO emission decreases at the outlet of the DPF system with the reciprocating cycle increasing in Table 5. The mean concentration of particulate matter, CO emission, HC emission and the mean pressure difference at the outlet of the DPF system are the average value of the parameters measured in 30 reciprocating flow cycles as the DPF system maintain stable operation at the reciprocating flow cycle set.

The variation of NO is associated with NO_2 during periodically reciprocating flow for every reciprocating cycle. At the beginning of each half cycle, the NO content decreases and the NO_2 content increases. As the NO content decreases to the troughs, the NO content increases with time. And as NO_2 content increases to the peaks, the NO_2 content begin to decrease. With the reciprocating cycle increasing, the fluctuating range of NO

and NO_2 components increases. But the change of the average NO and NO_2 components is not obvious.

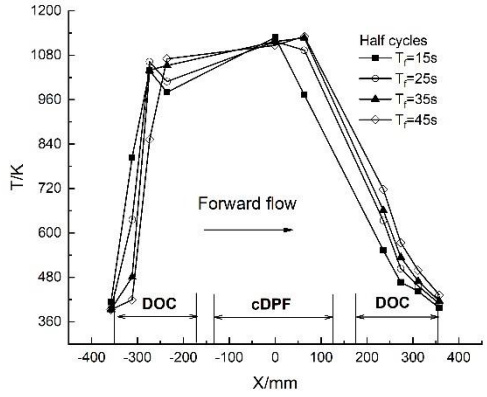

Figure 11. Influence of reciprocating cycles on temperature profiles

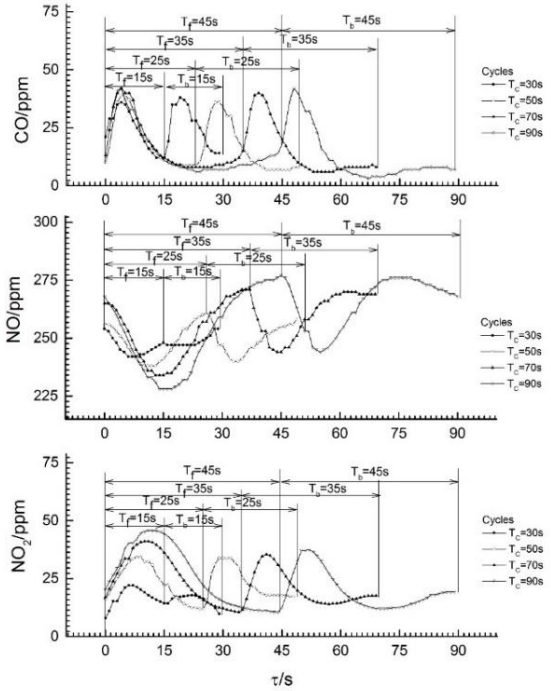

Figure 12. Profiles of CO、NO and NO_2 during different cycles

Table 5. Components of exhaust gas at the outlet of the DPF system

Cycle/s	O_2/%	CO/ppm	NO/ppm	NO_2/ppm	PM/mg/m^3	Δ P/Pa (with C_3H_8)	Δ P/Pa (without C_3H_8)
30	17.5	23.1	247.2	18.4	4.7	697.8	278.3
50	17.3	18.2	251.4	24.3	13.2	825.1	278.3
70	17.1	16.3	257.5	24.3	20.1	853.0	283.5
90	17.1	13.3	258.3	23.3	21.0	868.7	296.4

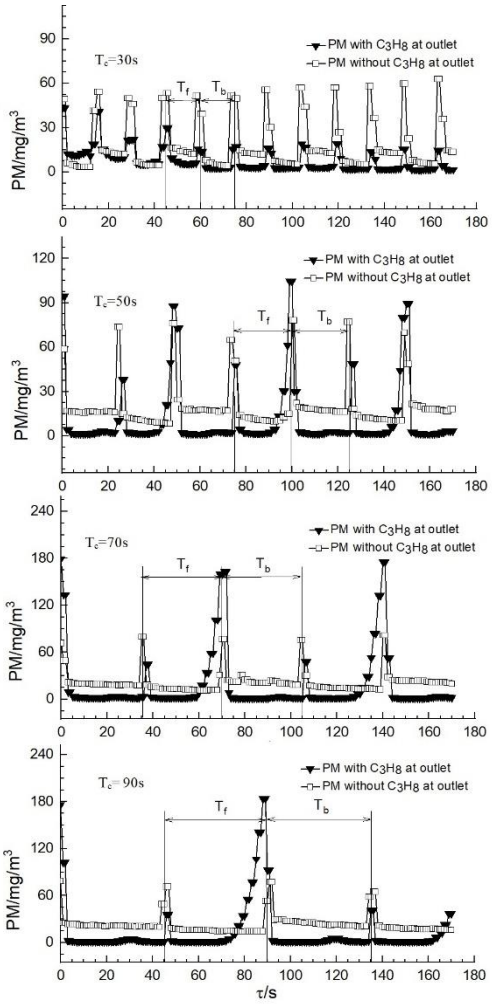

Figure 13. Profiles of PM at outlet for different reciprocating cycles

Figure 13 shows the corresponding profiles of PM components with and without C_3H_8 fuel addition at the outlet for different reciprocating cycles.

According to the published data in references 35, during each half cycle, no ashes are produced and deposited onto the internal walls to form an ash layer used as the substrate for particles deposition under the condition of no C3H8 fuel addition. The particles carried by the flow can be only deposited on the internal walls and hardly adhere to the internal walls. At the beginning of each half cycle after the flow direction immediately switched, the flow carrying the particles in the flow lines, the DOCs channels and in the inlet passages of cDPF reversely flow out the outlet of the DPF system for every reciprocating cycle. Most of residual particles deposited on the internal walls of the inlet passages during the previous T_f are stirred, blown

away and carried away by reverse flow immediately. Only a very small amount of the particles deposited on the internal walls during previous half cycle are blown away the internal walls and carried out the system by the reverse flow gradually. So, the PM content rapidly increases, rapidly decreases at the beginning of each half cycle, then and decreases gradually after the flow direction switched for every reciprocating cycles in Figure 13.

For 30s reciprocating cycle with C_3H_8 fuel addition, at the beginning of the half cycle, the temperature is lower than 623 *K* in upstream DOC, the chemical reaction equilibrium of NO_2 and NO is on the NO_2 side. The temperatures near the upstream end of the cDPF also keep lower than 823 K in Figure 11.The residual partial soot particles attached on the internal walls at rear part of the inlet passages or the outlet passages the during the previous half cycle are stirred and completely oxidized into ashes further with the NO_2 catalytic action. As switching to next half cycle, the PM content rapidly increases very low value and rapidly decreases in Figure 13. Because the reasonable temperature in upstream DOC and cDPF during each half cycle can be formed, the regeneration efficiency can be improved further in the reciprocating flow regeneration process of the DPF system, compared with that of 50s reciprocating cycle noted above. For 30s reciprocating cycle, the average PM content at the outlet of the system is only 4.7 mg/m^3.

For 50s, 70s and 90s reciprocating cycle with C3H8 fuel addition, only at the beginning of the T_b, the temperature is lower than 623 *K* in upstream DOC, the chemical reaction equilibrium of NO_2 and NO is on the NO_2 side. The temperatures near the right end of the cDPF also keep lower than 823 K in Figure 13. The residual partial soot particles attached on the internal walls at rear part of the inlet passages during the previous T_f are stirred and completely are oxidized into ashes further with the NO_2 catalytic action. Because the temperature profile moves toward the downstream side during the T_f with the reciprocating cycle increasing, that results to the higher temperature than 623 *K* in the partial region of the downstream DOC. And the conversion rate from NO to NO_2 decreases in new upstream DOC during the T_b with the reciprocating cycle increasing. The regeneration efficiency of the DPF system decreases and the average content of PM emission increases with the reciprocating cycle increasing.

The efficiency of removing particulates of the DPF system is over 95%, the pressure difference is less

than 1100 Pa, the CO emission is less than 20 ppm and the HC emission is near zero for every reciprocating flow cycle set in the experiment.

■ CONCLUSIONS

An experimental study on the characteristics of removing pollution emissions and regeneration of the DPF system with reciprocating flow has been carried out. The influence of reciprocating flow cycle on the regeneration procedure of the DPF system has been also analyzed.

(1) After stared up, the DPF system with reciprocating flow can use a tiny amount of extra fuel to maintain the chemical reaction, releasing and storing heat periodically, blow away ash and realize the continuous regeneration of the cDPF.

(2) If the reasonable temperature in upstream DOC and cDPF during one half cycle is formed, the regeneration efficiency can be improved in the reciprocating flow regeneration process of the DPF system.

(3) The reciprocating cycles of the DPF system can influence the operation performance of DPF system. With the reciprocating cycle increasing, the temperature profile moves parallel toward the downstream side and the fluctuating range of CO、NO and NO_2 components increases.

(4) If the reasonable temperature in upstream DOC and cDPF during each half cycle is formed, the regeneration efficiency of the DPF system can be obviously improved. For 30s reciprocating cycle the average content of PM emission at the outlet of the DPF system is only 4.7 mg/m^3.

■ AUTHOR INFORMATION

Corresponding Author. Tel:86-0411-84725295. E-mail: dengyb@dlmu.edu.cn

Author Contributions. The manuscript was written through contributions of all authors. All authors have given approval to the final version of the manuscript.

Notes. The authors declare no competing financial interest.

■ ACKNOWLEDGEMENTS

Our work in this paper has been supported in part by Coal Joint Fund of the National Natural Science Fund Committee of China - Shenhua Group Corporation Ltd. (NSFC Grant Nos. U1361111) and the Fundamental Research Funds for the Central Universities of China (Grant No. 3132016340).

■ ABBREVIATIONS

c_s, specific heat capacity of solid phase [$Jkg^{-1}K^{-1}$]; ΔP, differential pressure [Pa]; q_R, heat release per unit time in solid frame [Js^{-1}]; q_S, heat storage per unit time in solid frame [Js^{-1}]; Q_R, heat release in solid frame [J]; Q_S, heat storage in solid frame [J]; T, temperature, [K]; T_b , backward half cycle [s]; T_c, the reciprocating flow cycle, [s], T_f , forward half cycle, [s]; T_{l1}, light off temperature of soot in loose contact [K]; T_{l2}, light off temperature of soot in intimate contact [K]; T_{sof} , the discharge temperature of SOF [K]; X, position along the axis of the DPF system [mm]; τ, time [s]; ρ_s, solid density [kgm^{-3}]

■ REFERENCES

(1) Neeft, J.P.A.; Makkee, M.; Moulijn, J.A. Diesel particulate emission control. Fuel Process Technol. 1996,47,11.

(2) Vouitsis, E.; Ntziachristos, L.; Samaras, Z. Particulate matter mass measurements for low emitting diesel powered vehicles: what's next? Prog. Energy Combust. Sci. 2003,29,635.

(3) Francesco, D.N.; Claudia, C. Particulate matter in marine diesel engines exhausts: Emissions and control strategies. Transport. Res.D-TR.E. 2015,40,166.

(4) Zhang, Y.H.; Lou, D.M.; Tan, P.Q.; Hu, Z.H. Experimental study on the particulate matter and nitrogenous compounds from diesel engine retrofitted with DOC+CDPF+SCR. Atmos. Environ. 2018,177,45.

(5) Burtscher, H. Physical characterization of particulate emissions from diesel engines: a review. Aerosol. Sci. 2005,36,896.

(6) Guan, B.; Zhan, R.G.; Lin, H.; Huang, Z. Review of the state-of-the-art of exhaust particulate filter technology in internal combustion engines. J. Environ. Manage. 2015,154,225.

(7) Grigoratos, T.; Fontaras, G.; Giechaskiel, B.; Zacharof, N. Real world emissions performance of heavy-

duty Euro VI diesel vehicles. Atmos. Environ. 2019,201,348.

(8) Ko, J.; Myung, C.-L.; Park, S. Impacts of ambient temperature, DPF regeneration, and traffic congestion on NOx emissions from a Euro 6-compliant diesel vehicle equipped with an LNT under real-world driving conditions. Atmos. Environ. 2019,200,1.

(9) Jeguirim, M.; Tschamber, V.; Brilhac, J.F.; Ehrburger, P. Oxidation mechanism of carbon black by NO_2: effect of water vapour. Fuel 2005,84,1949.

(10) E, J.Q., Zhao, X.H.; Xie, L.F.; Zhang, B.; Chen, J.W.; Zuo, Q.S.; Han, D.D.; Hu, W.Y.; Zhang, Z.Q. Performance enhancement of microwave assisted regeneration in a wall-flow diesel particulate filter based on field synergy theory. Energy 2019,169,719.

(11) Ibrahim, A.R.; Kemal, A.S.; Ali, K. The pollutant emissions from diesel-engine vehicles and exhaust aftertreatment systems, Clean. Techn. Environ. Policy 2015;17:15–27.

(12) Mohankumara, S.; Senthilkumar, P. Particulate matter formation and its control methodologies for diesel engine: A comprehensive review. Renew. Sust. Energ. Rev. 2017,80,1227.

(13) Jiao, P.H.; Li, Z.J.; Li, Q.; Zhang, W.; He, L.; Wu, Y. Simulation of low temperature combustion mechanism of different combustion-supporting agents in close-coupled DOC and DPF system. ISA T. 2018,78,88.

(14) Zhang, Y.H.; Lou, D.M.; Tan, P.Q.; Hu, Z.Y. Experimental study on the particulate matter and nitrogenous compounds from diesel engine retrofitted with DOC+CDPF+SCR. Atmos. Environ.2018,177,45.

(15) Yu, M.T., Luss, D. Inlet Cone Effect on Particulate Matter Deposition and Regeneration Temperature in a Diesel Particulate Filter. Ind. Eng. Chem. Res. 2012,51,3791.

(16) Caliskan, H.; Moric, K. Environmental, enviroeconomic and enhanced thermodynamic analyses of a diesel engine with diesel oxidation catalyst (DOC) and diesel particulate filter (DPF) after treatment systems. Energy 2017,128,128.

(17) Ning, J.B.; Yan, F.J. Composite Control of DOC-out Temperature for DPF regeneration. 8th IFAC International Symposium on Advances in Automotive Control, June 19-23, 2016. Norrköping, Sweden.

(18) Fang, J.; Meng, Z.W.; Li, J.S.; Du Y.H.; Qin Y.; Jiang, Y.; Bai, W.L.; George, G.C. The effect of operating parameters on regeneration characteristics and particulate emission characteristics of diesel

particulate filters. Appl. Therm. Eng. 2019,148,860.

(19) Zhang, J.; Wong, V.W.; Shuai, S.J.; Chen, Y.; Sappok, A. Quantitative estimation of the impact of ash accumulation on diesel particulate filter related fuel penalty for a typical modern on-road heavy duty diesel engine. Appl. Energ. 2018,229,1010.

(20) Fang, J.; Meng, Z.W.; Li, J.; Pu, Y.F.; Du, Y.H.; Li, J.S.; Jin, Z.X.; Chen, C.; George, G.C. The influence of ash on soot deposition and regeneration processes in diesel particular filter. Appl. Therm. Eng. 2017,124,633.

(21) Wang Y.J; Pan, YL; Su, C.S.; Srinivasan, A.; Gong, J.; Carl, J. K. Performance of Asymmetric Particulate Filter with Soot and Ash Deposits: Analytical Solution and Its Application. Ind. Eng. Chem. Res. 2018, 57,15846.

(22) Konstandopoulos, A. G.; Kostoglou, M. Reciprocating flow regeneration of soot filters, Combust. Flame 2000, 121,488.

(23) Zheng, M.; Banerjee, S. Diesel oxidation catalyst and particulate filter modeling in active – Flow configurations. Applied Thermal Engineering, 2009, 29, 3021.

(24) Zheng, M,; Wang, D.; Reader, G.T. Boundary Layer Enhanced Thermal Recuperation for Diesel Particulate Filter Regeneration under a Periodic Flow Reversal Operation, SAE technical paper 2005-01-0951, 2005.

(25) Reader, G.T.; Banerjee, S.; Wang, M.; Zheng, M. Energy Efficiency Analysis of Active-flow Operations in Diesel Engine Aftertreatment, SAE 2006-01-3286, 2006.

(26) Moffat, R.J. Describing the uncertainties in the experimental results. Exp. Therm. Fluid Sci. 1988,1,3.

(27) Mollenhauer, K.; Tschöke, H. Handbook of diesel engines, Springer, Berlin,Germany,2010.

(28) Johansen, K. Multi-catalytic soot filtration in automotive and marine applications. Catal. Today 2015,258,2.

(29) Southward, B.W.L.; Basso, S. An Investigation into the NO_2-decoupling of Catalyst to Soot Contact and its Implications for Catalyzed DPF Performance. SAE Int. J. Fuels Lubr. 2009,1,239.

(30) Southward, B.W.L.; Basso, S.; Pfeifer, M. On the Development of Low PGM Content Direct Soot Combustion Catalysts for Diesel Particulate Filters. SAE Technical Paper 2010-01-0558, 2010.

(31) Xu, G.J.; Li, M.D.; Zhao, Y. Basic theory of the diesel engine particulate emission, Jiangsu university press, Zhanjiang, China,2017.

(32) Torregrosa, A.J.; Serrano, J.R.; Piqueras, P. Oscar GA. Experimental and computational approach to the transient behavior of wall-flow diesel particulate filters. Energy 2017,119,887.

(33) Choi, S.; Oh, K.C.; Lee, C.B. The effects of filter porosity and flow conditions on soot deposition/oxidation and pressure drop in particulate filters. Energy 2014,77,327.

(34) Kong, X.J.; Li, Z.J.; Shen, B.X; Wu,Y.; Zhang,Y.K.; Cai,D. Simulation of flow and soot particle distribution in wall-flow DPF based on lattice Boltzmann method. Chemical Engineering Science 2019, 202, 169.

(35) Anthi, L.; Panayotis, D.E. Characterization of particulate matter deposited in diesel particulate filters: Visual and analytical approach in macro-, micro- and nano-scales. Combustion and Flame 2010,157, 1658.

TOC/Abstract Graphics